

# Effective Reduction of CSF Partial Volume Effect in DTI by Acquiring Additional DWIs with Smaller B-value

E. S. Hui<sup>1,2</sup>, J. A. Helpert<sup>3,4</sup>, and E. X. Wu<sup>1,2</sup>

<sup>1</sup>Laboratory of Biomedical Imaging and Signal Processing, The University of Hong Kong, Hong Kong SAR, China, People's Republic of, <sup>2</sup>Electrical and Electronic Engineering, The University of Hong Kong, Hong Kong SAR, China, People's Republic of, <sup>3</sup>Department of Radiology, New York University School of Medicine, New York, NY 10016, United States, <sup>4</sup>Centre for Advanced Brain Imaging, The Nathan Lkine Institute, Orangeburg, NY 10962, United States

## Introduction

One of the major limitations of conventional DTI is its vulnerability to CSF. Approaches have been proposed to remove CSF partial volume effect by using fluid-attenuated inversion recovery (FLAIR) preparation prior to acquisition (1-3), or using a two-compartment tensor model for acquisition and analysis (4). However, they substantially increase scan time (and lead to SNR reduction in the former case). A simple and effective approach to eliminate fluid contamination in DTI is proposed in the current study. DT is computed from diffusion-weight images (DWIs) acquired with a regular b-value and a smaller one along each diffusion encoding direction. Conventional diffusion tensor (DT) is also computed from  $b_0$  and DWIs with  $b=1000\text{s/mm}^2$ . DT-derived parametric maps from the proposed method are compared with those computed from conventional DTI data.

## Methods

**Human experiments** were performed on a 3T Siemens MR system on 3 normal subjects (ages 16–44 yrs). DWIs were acquired using dual SE EPI with 30 gradient directions and 5  $b_0$  (5) using: TE/TR=108/2300ms,  $\delta/\Delta=34.5/36.1\text{ms}$ , FOV=256x256mm<sup>2</sup>, resolution=2x2x2mm<sup>3</sup>, 2 b-values of 500 and 1000s/mm<sup>2</sup> and NEX=2. **Animal experiments** were performed in 4 normal SD rats in vivo using a 7T Bruker scanner. DWIs were acquired with a respiration-gated SE 4-shot EPI with the same directions and b-values as in human scans, and using: TE/TR=30.3/3000ms,  $\delta/\Delta=5/17\text{ms}$ , resolution = 313x313x1000 $\mu\text{m}^3$  and NEX=1. Conventional DT (cDT) was computed from  $b_0$  and DWIs with  $b=1000\text{s/mm}^2$ . The proposed fluid-suppressed DT (fsDT) was calculated from DWIs with b-values of 500 and 1000s/mm<sup>2</sup>. FA, mean and directional diffusivity (MD,  $\lambda_{//}$  and  $\lambda_{\perp}$ ) maps were obtained. Percentage difference maps were also computed between cDT- and fsDT-derived maps. WM and GM tissues were segmented based on conventional FA (cFA) and  $\lambda_{\perp}$  ( $\lambda_{\perp}$ ) maps for quantitative measurements.

## Results

Fig.1 compares the typical FA, MD,  $\lambda_{//}$  and  $\lambda_{\perp}$  maps obtained from cDT and fsDT in one volunteer, together with WM and GM segmentation masks. Substantial differences in contrast are observed between the two sets of maps, especially in regions near the cortical surface and ventricles. The percentage difference maps are shown in Fig.2. GM and WM measurements from all volunteers are given in Table 1. Note that, using the proposed fsDT, diffusivities are lower and FA are higher in both WM and GM. Interestingly, CSF has a larger effect on  $\lambda_{\perp}$  than  $\lambda_{//}$  in GM structures, as demonstrated by a larger  $\lambda_{\perp}$  decrease. Animal results are also shown in Fig.3, again illustrating the CSF signal reduction using the proposed fsDT approach (and changes of mean and directional diffusivities in different neural structures – not shown).

## Discussions and Conclusions

The results suggest that, by computing DT using DWI with b-values of 500 and 1000s/mm<sup>2</sup>, CSF can be effectively suppressed. At a b-value of 500s/mm<sup>2</sup>, the CSF signal is reduced by 88% in  $b_0$  images while SNR is maintained in brain tissues given that CSF MD is  $\sim 3 \times 10^{-3}\text{mm}^2/\text{s}$  in vivo. Note that the absolute percentage differences between cDT- and fsDT-derived parameters will depend on a number of factors that affect the CSF partial volume effect and CSF signal reduction, including voxel resolution and actual b-values used.

The proposed fsDT approach requires nearly twice the scan time as in conventional DTI. In high angular resolution DTI, this limitation may be alleviated by using the minimal number of diffusion encoding directions for the lower b-value. Optimal choice of the low b-value remains to be determined, depending on SNR efficiency and the amount of fluid or fast-diffusing water suppression desired. Also note that non-monoexponential b-value dependency has been observed in DW signal for various neural tissues due to the complex cellular microstructures and restricted diffusion processes. Use of different b-values may lead to different sensitivity in probing these structures and events.

In conclusion, our results indicate that the proposed 2 b-value approach is effective in reducing the CSF partial volume effect. The approach can lead to more accurate DTI quantitation, which can improve DTI sensitivity and specificity in detecting pathological changes in both brain tissues.

## References

- [1] Latour LL et al. Magn Reson Med 2002;48(3):478-486.
- [2] Falconer JC et al. Magn Reson Med 1997;37(1):119-123.
- [3] Papadakis NG et al. Magn Reson Med 2002;48(2):394-398.
- [4] Pierpaoli C et al. ISMRM 2004, Kyoto, Japan. p1215.
- [5] Jones DK et al. Magn Reson Med 1999;42(3):515-525.

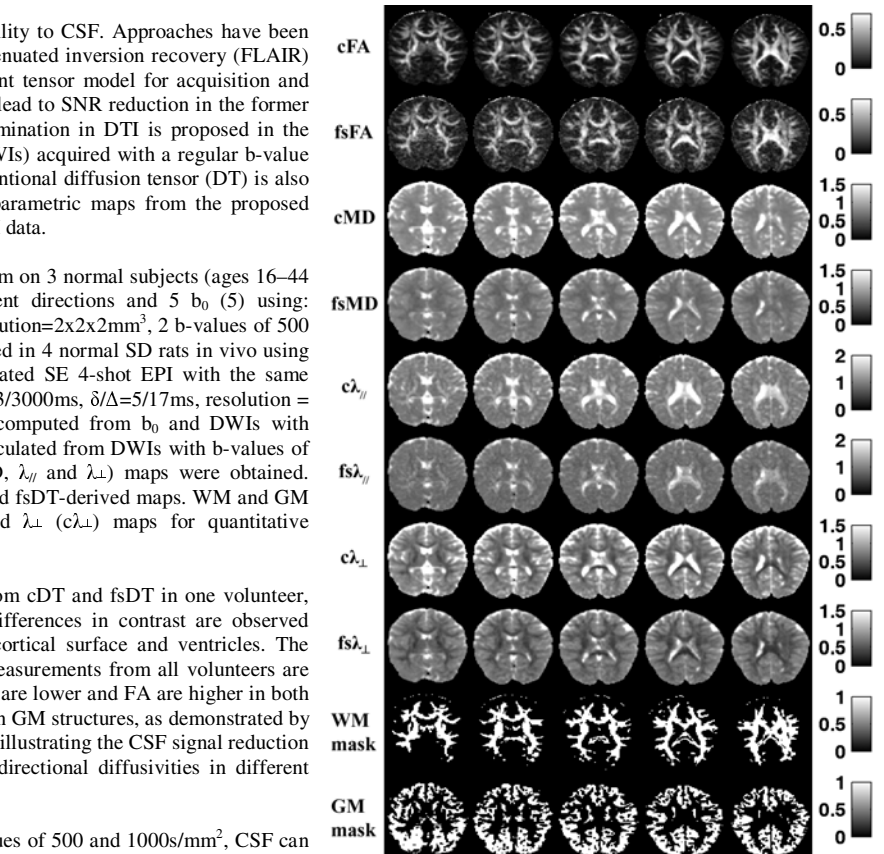


Fig.1 Typical cDT- and fsDT-derived parametric maps in a volunteer, and WM and GM masks for quantitation.

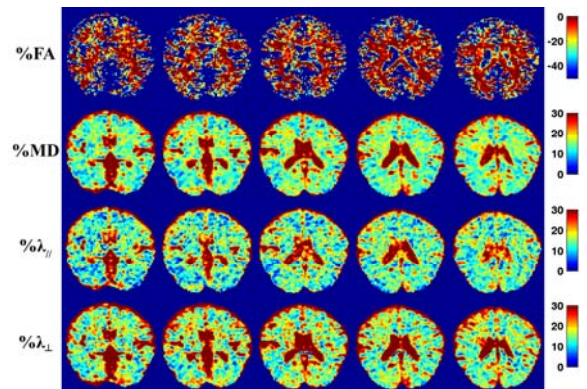


Fig.2 Percentage difference maps in the same volunteer (between cDT- and fsDT-derived maps).

	GM	WM
FA	-28.80 ± 3.26%	-3.15 ± 0.23%
MD	16.03 ± 3.01%	17.76 ± 2.53%
$\lambda_{//}$	13.66 ± 2.95%	17.10 ± 2.67%
$\lambda_{\perp}$	17.44 ± 3.07%	18.37 ± 2.42%

Table 1. Measurements of percentage difference between cDT- and fsDT-derived parameters in 3 human subjects. Data are presented as mean±SD.

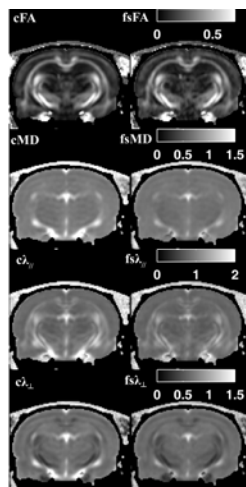


Fig.3 Typical cDT- and fsDT-derived maps in a normal SD rat in vivo.